22. Nachwuchswissenschaftler*innenkonferenz (NWK)
https://doi.org/10.52825/ocp.v2i.132

Published: 15 Dec. 2022

Analysis of the compression behavior of different cardboard materials during embossing

Ulrike Kaeppeler[1*], Klaus Schneller[2], Florian Wallburg[2], Lutz Engisch[1], and Stephan Schoenfelder[2]

[1] Leipzig University of Applied Sciences, Faculty of Computer Science and Media, Institute for Printing, Processing and Packaging, Germany

[2] Leipzig University of Applied Sciences, Faculty of Engineering, Germany

[*] Corresponding author: ulrike.kaeppeler@htwk-leipzig.de

Abstract. Embossing is an important design and functionality element. For instance, embossing is used to apply braille letters on medical products, or to enhance folding packages or brochures due to haptic effects. Usually, a multilayered cardboard material is used for such types of products. Up to now, high-quality and functional embossing has so far been associated with an extraordinarily large amount of experience-based know-how and with many cost-intense trial-and-error experiments due to the mechanical complexity of cardboard material. In the presented work it is shown how experimental investigations and numerical simulations based on Finite-Element-Analysis can contribute to a virtual prediction of the embossing process and, therefore, can help to reduce time-consuming and expensive experiments.

1. Introduction

Nowadays, embossings are mainly created according to the trial-and-error principle. Employees with a high level of experience supervise the process from the selection of the material, over the creation of the tools, up to testing and delivery to the customer. However, the state of mechanical knowledge regarding the process of embossing itself is very limited so far, as it is a complex interaction between material, machine, tools and environmental conditions. A decisive factor for the embossing result is the compression behavior of the cardboard.

Fibrous materials, such as cardboard, have different layers and masses per unit area. Often the surface is covered with a coating. In most cases, this serves to smooth the surface and is important for further processing (printing, cutting, embossing). Fibers commonly used consist of 40 % cellulose, 30 % hemicellulose and 20 to 30 % lignin having again a structure that is composed of individual fibers of different lengths, widths, angles etc. [1; 2; 3]. Between the fibers there are either voids or fillers such as calcium carbonate or kaolin. The basis of the paper fibers (and, thus, for the paper strength) are hydrogen bonds [4; 5].

To obtain information about the compression behavior of different cardboards, a compression test is used in the presented study. During the test, a force is applied to the sample via a stamp. As the compression distance increases, the force increases exponentially until the material is fully compressed. The compression process is as follows: First, the roughness peaks are levelled out [6]. This requires a relatively small amount of force. For paper and cardboard, the Rz value is approximately 12 µm [7]. This is followed by the compression of the fiber structure and the elimination of the voids until the material is completely compacted.

The compression of the voids is followed by the compression of the fibers itself in the fiber structure. This significantly increases the force required for further compression. Compression is especially crucial for the forming process of embossing, nevertheless there is little research that describe the compression behavior numerically.

Due to the manufacturing process and the low thickness of the material, cardboard shows strongly anisotropic behavior in the plastic regime, which can be described by the Hill Yield Criterion [8]. In general, this model is applicable to materials with relatively small differences in yield stresses between the respective directions – which is not the case for cardboard [9]. Therefore, calculation approaches have been published trying to avoid this problem by completely uncoupling the thickness direction from the in-plane directions. As a consequence, only two-dimensional material models are obtained [10; 11]. This work shows a way of modeling the compaction behavior of cardboard using a three-dimensional Hill plasticity model, which provides the ability to analyze the full stress/strain state inside the material.

2 Experimental

2.1 Experimental Set up

Two different cardboard materials were used for the investigation. Fig. 1 shows an overview of the composition and its differences.

Material **B3-230 and B3-330**	**Things in common**	**Differences**
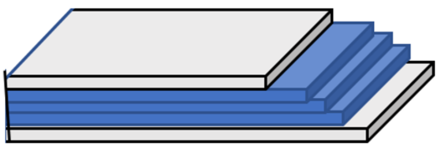 outer layers: coating inner layers: fiber layers	3 layers double sided coating chemical pulp – therefore no lignin content	Mass per unit area B3-230: 230 g/m2 B3-330: 330 g/m2 Material thickness B3-230: 256 µm B3-330: 400 µm

Figure 1: Cardboard materials B3-230 and B3-330 used in the experiment

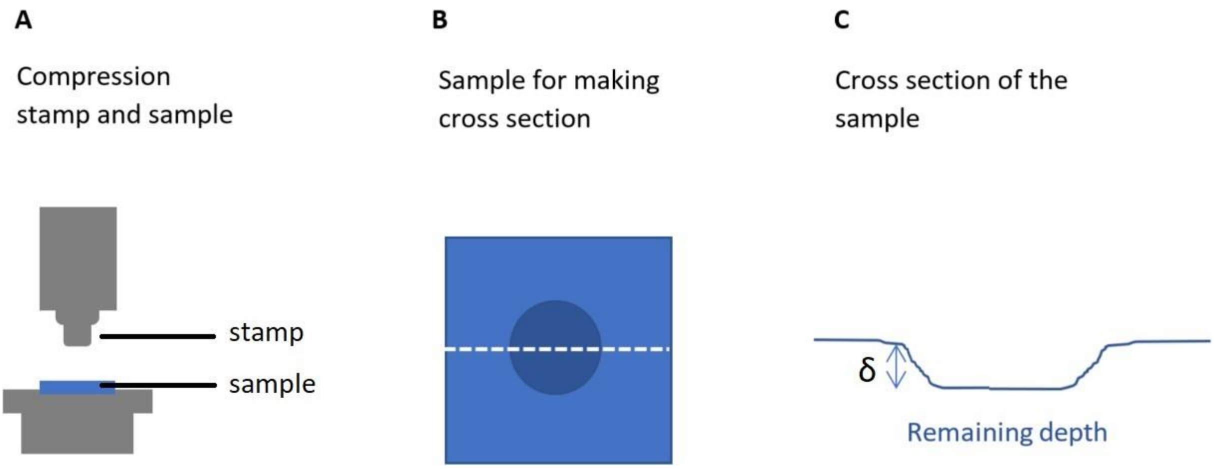

Figure 2: A: Measurement setting for measuring the compressibility of cardboard and B: Place of the virtual cross section and C: Cross section for measuring the resulting material thickness

To investigate the compressibility, the material thickness is first measured with a thickness gauge prior to compression (Frank Dickenmesser, Germany). An universal testing machine (ZwickRoell, Ulm, Germany) with a compression module is further used to investigate the compression behavior. Fig. 2 A shows the experimental set-up.

The compression module consists of a stamp with a circular test surface. Because of the round geometry, the stamp has a surface area of 100 mm^2 with a 1 mm rounding at the edge. The material is located on the counter-pressure stamp. The material is compressed at a constant speed of 5 mm/min until the test ends when the upper force limit of 15000 N is reached. Under this load, the material may be assumed as fully compressed. During the process, the force and the compression displacement are recorded to calculate the resulting material thickness under load.

With the help of a Keyence 3D macroscope (Keyence Germany GmbH, Neu-Isenburg, Germany), the resulting material thickness can be measured after pressure release. This is done by measuring the surfaces of the samples using the fringe light projection technique capturing height information of the samples. By means of a virtual cross-section through the compressed area, the resulting height of the compressed material can be determined. Fig. 2 B and C show the measurement process schematically. As shown in Fig. B, a vertical (and a horizontal) cross-section are conducted. In the resulting profile section (Fig. 2 C), the characteristic value δ, which denotes the *remaining indentation depth* is shown.

2.2 Numerical approach

Due to its fibrous structure, cardboard shows an orthotropic behavior in the elastic regime, leading to nine independent material parameters (three elastic moduli, poisson ratios and shear moduli respec- tively). For the compaction behavior, the elastic module in thickness direction (ZD) is of outstanding interest and can be derived from the described experiment. As mentioned before, anisotropic plasticity is often modeled using the Hill Yield Criterion, which is a general extension of the von Mises Criterion. The function of the yield surface is given in Eq. (1). σ_{ij} represents the actual stress state and the coefficients F, G, H, L, M, N contain the yield stresses along the three principle axes and shear planes, respectively:

$$F(\sigma_{22}-\sigma_{33})^2+G(\sigma_{33}-\sigma_{11})^2+H(\sigma_{11}-\sigma_{22})^2+2L(\sigma_{23})^2+2M(\sigma_{31})^2+2M(\sigma_{12})^2-1=0 \quad (1)$$

The values used here were obtained by Coffin et al. [13]. They can be found in Table 1.

Table 1: Elastic and plastic parameters used for the simulation model

Elastic Parameter	E_x	E_y	E_z	G_{xy}	G_{yz}	G_{xz}	ν_{xy}	ν_{yz}	ν_{xz}
Value [MPa] resp. [-]	6000	3000	100	2000	100	100	0,2	0,02	0,01
Plastic Parameter	F	G	H	L	M	N			
Value [10^{-3}]	6,3542	3,6458	-1,9097	1,3889	1,0035	5,8681			

However, this yield criterion is independent of volumetric stresses/strains and, therefore, in its original form inadequate to model compaction of a material. In order to cover the compaction behavior of cardboard under compressive stresses, an additional compaction criterion, shown in Eq. (2), is introduced

$$\text{If} \quad \sigma_{33} < \sigma_{\text{comp}} \quad \text{then} \quad \varepsilon_{\text{pl},11} = \varepsilon_{\text{pl},22} = 0 \quad (2)$$

where σ_{comp} gives the actual stress during the compaction process and $\varepsilon_{\mathrm{pl},ii}$ are the plastic strains along the principal axes (first invariant of plastic strain tensor). As described in Sec. 2.1, the force rises exponentially during compaction of the material, while the maximum achievable compressibility is limited. This behavior is modeled with an exponential strain hardening approach and an increasing elastic modulus in z-direction, E_{z}, due to the compression of the fiber structure and the associated higher stiffness. The evolution of these two properties is shown in Eq. (3) and (4):

$$\sigma_{\mathrm{comp}} = \sigma_{\mathrm{comp},0} \cdot e^{a \cdot |\varepsilon_{\mathrm{pl,zz}}|} \tag{3}$$

$$E_{\mathrm{z}} = E_{\mathrm{z},0} \cdot e^{b \cdot |\varepsilon_{zz}|} \tag{4}$$

where the index 0 implies the beginning of the compaction process. The parameters used for the compaction model are fitted from some other type of folding cardboard with a thickness of ca. 367 µm and are shown in Table 2. By choosing the parameters *a* > *b*, it is ensured that the hardening modulus increases faster than the elastic modulus and, thus, plastic strain of the material is limited. The simulation is conducted with a displacement-driven scenario up to 45 % strain.

Table 2: Used material parameters for the compaction model

Parameter	$\sigma_{\mathrm{comp},0}$ [MPa]	a	$E_{\mathrm{z},0}$ [MPa]	b
Value	20	8	60	6,8

3. Results and discussion

3.1 Material Thickness under Load

To determine the material thickness under load, the compression way was determined with the Zwick Universal testing machine. The compression way corresponds to the penetration depth of the tool into the material. Fig. 3 shows the force-displacement-data obtained from the experiment as well as from the simulation.

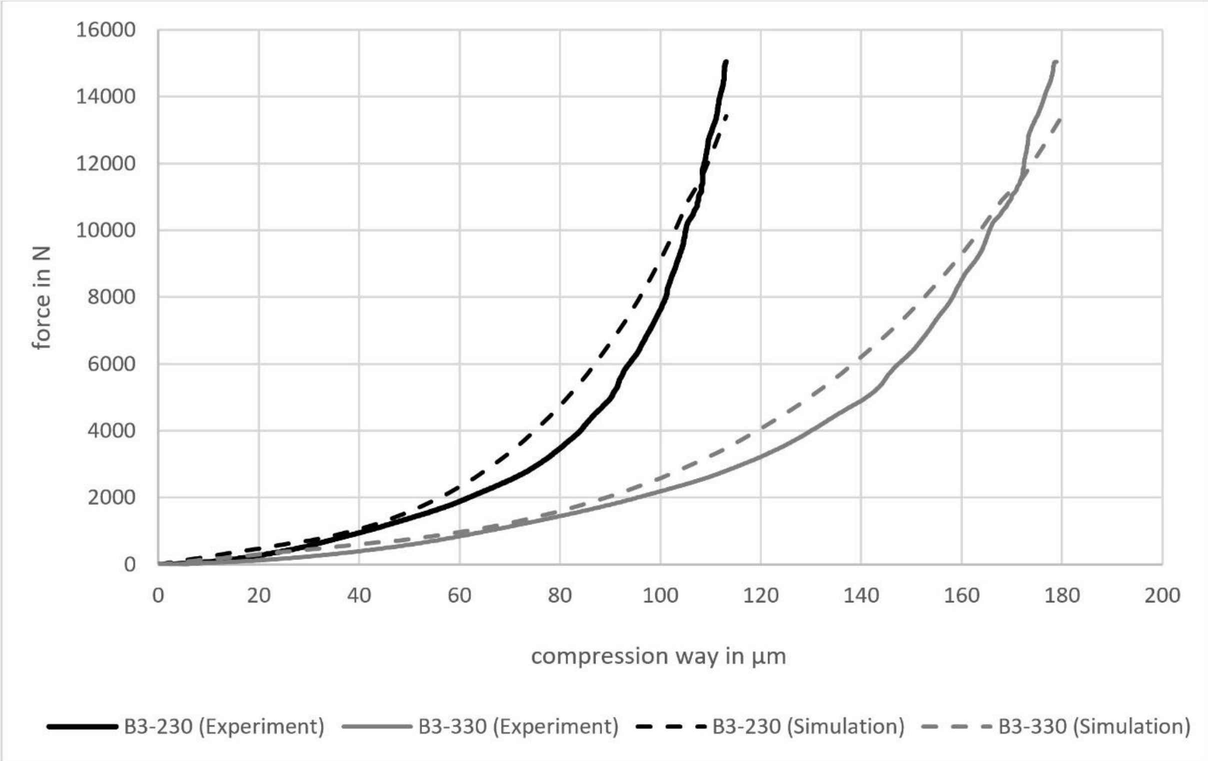

Figure 3: Force-displacement (compression way) diagram during the compression process

It can be seen from Fig. 3 that the force increases exponentially with increasing penetration depth. Due to their different material thicknesses, the two types of cardboard materials differ mainly in their maximum specific penetration depth, while the shape is similar. The simulation results agree reasonably well with the experimental data, but tend to underestimate the force towards the end of the compaction process. Due to the high stiffness of the material at the end of the process, achieving convergence is an issue. The results containing the information about the permanent displacement of the cardboard are presented in the following section.

3.2 Material Thickness after Pressure Relief

To determine the resulting material thickness after the process, the samples were taken out of the compression tool. They were then measured optically using fringe light projection. The penetration depth after pressure release could be calculated with a virtual profile section. The values for both cardboard materials are shown in Fig. 4 A. In both cases the material thickness after pressure release is significantly higher than the one under pressure. This is due to the elastic part of the displacement, which is recovered after releasing the pressure.

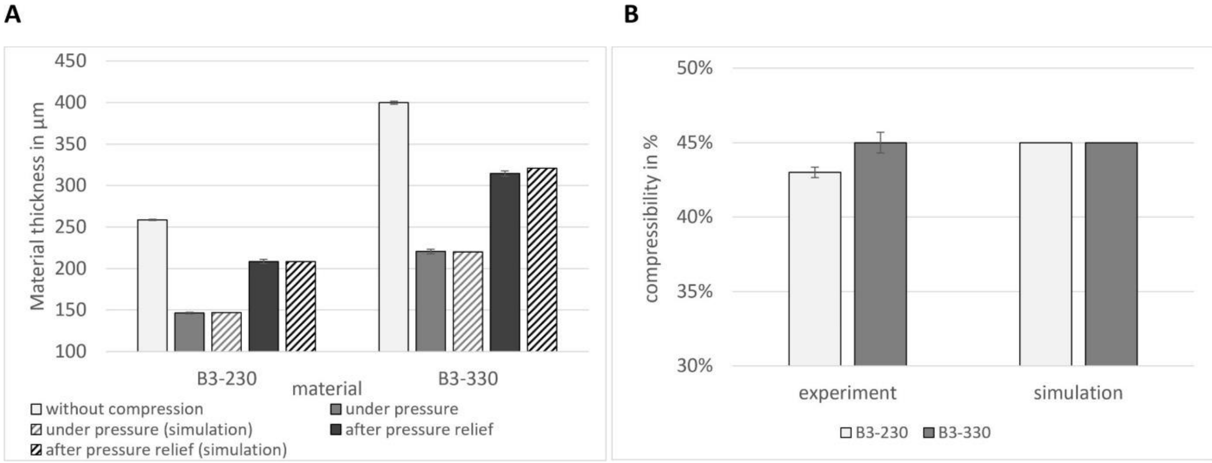

Figure 4: Experimental and numerical results - A: thickness of material in loaded and unloaded state and B: relative compressibility

To compare the compressibility of different cardboards and/or different grammages, the relative compressibility can be used. It is defined as the ratio of permanent displacement and initial material thickness. These results are shown in Fig. 4 B. The diagram shows that both times the compressibility is around 45 %. As expected, the relative compressibility of the thinner material does not differ significantly from that of the thicker material. Since the material model works with fixed parameters, the numerical result is the same for both cardboard material. Although this approach is well suited for the used cardboard materials, however, validation/re-determination of the parameters regarding other types of cardboard, e.g. for materials without coatings, should be subject of future research.

4 Summary

A high-quality and undamaged embossing is a result of many experimental efforts and a lot of practical knowledge. Digital technologies like numerical simulations can help to improve this economically and ecologically demanding process, but require a profound mechanical understanding of the material. The investigations presented here focused primarily on the compaction behavior of cardboard during the embossing process. Together with the first approaches of a material model for cardboard, it could be shown that it is numerically possible to adequately predict the compression behavior of the two types of cardboard tested. In subsequent works, the presented model will be extended to more extensive embossing processes and patterns in order to be able to further accelerate the digitalization of the embossing industry.

Data availability statement

Access to all data can be requested from the authors in individual cases.

Competing interests

The authors declare that they have no competing interests.

Acknowledgement

This work has been financially supported by the Saxonian Ministry of Science and Arts as well as the European Union within the research project SmartKMU (Project No. 100 38 21 59), which are gratefully acknowledged.

References

1. Bayerl, G., Pichol, K., 1986. Papier: Produkt aus Lumpen, Holz u. Wasser. volume 7727 of Kulturgeschichte der Naturwissenschaften und der Technik. Rowohlt, Reinbek bei Hamburg.
2. Ek, M., Gellerstedt, G., Henriksson, G., 2009. Wood chemistry and wood biotechnology. volume 1 of Pulp and paper chemistry and technology. DE GRUYTER, Berlin.
3. Franke, W. (Ed.), 1993. Prüfung von Papier, Pappe, Zellstoff und Holzstoff: Teil 3: Physikalisch-technologische Prüfung. Springer, Berlin and Heidelberg.
4. Radzanowski, G., 2017. Untersuchungen zu Strukturveränderungen in Karton im ultraschallun-terstützten Prägeprozess. Masterarbeit. Hochschule für Technik, Wirtschaft und Kultur Leipzig. Leipzig.
5. Brenner, T., 2016. Anwendung von Ultraschall zur Verbesserung der Papierfestigkeit durch Beeinflussung der Fasermorphologie. volume 17 of Schriftenreihe Holz- und Papiertechnik. TU Dresden, Institut für Naturstofftechnik, Professur für Papiertechnik, Dresden.
6. Schaffrath, H.J., 1992. Modellierung der Kompression von Papier in z-Richtung bei niedriger Flächenpressung. Das Papier.
7. Käppeler, U., 2019. Charakterisierung physikalisch-chemischer Veränderungen im Karton im ultra-schallunterstützten Prägeprozess. Hochschule für Technik, Wirtschaft und Kultur Leipzig, Leipzig.
8. Hill, R., 1948. A theory of the yielding and plastic flow of anisotropic metals. Proc. Roy. Soc. London 193, 281–297.
9. De Borst, R., Feenstra, P.H., 1990. Studies in anisotropic plasticity with reference to the hill criterion. International Journal for numerical methods in engineering 29, 315–336.
10. Xia, Q.S., 2002. Mechanics of inelastic deformation and delamination in paperboard. Dissertation. Massachusetts Institute of Technology. Atlanta.
11. Nygårds, M., Just, M., Tryding, J., 2009. Experimental and numerical studies of creasing of paperboard. International Journal of Solids and Structures 46, 2493–2505. doi: https://doi.org/10.1016/j.ijsolstr.2009.02.014.
12. Coffin, D.W., Gustafsson, P.J., Hägglund, R., Kulachenko, A., Mäkelä, P., Nygards, M., Östlund, S., Uesaka, T., Niskanen, K., Berglund, L., Carlsson, L.A., 2011. Mechanics of Paper Products. DE GRUYTER, Berlin, Boston. doi: https://doi.org/10.1515/9783110254631.